

This is an Open Access document downloaded from ORCA, Cardiff University's institutional repository: <https://orca.cardiff.ac.uk/id/eprint/139365/>

This is the author's version of a work that was submitted to / accepted for publication.

Citation for final published version:

Hernandez, Juan D. , Sanz, David, Rodríguez-Canosa, Gonzalo R., Barrientos, Jorge, del Cerro, Jaime and Barrientos, Antonio 2013. Sensorized robotic sphere for large exterior critical infrastructures supervision. *Journal of Applied Remote Sensing* 7 (1) , 073522. 10.1117/1.JRS.7.073522

Publishers page: <http://dx.doi.org/10.1117/1.JRS.7.073522>

Please note:

Changes made as a result of publishing processes such as copy-editing, formatting and page numbers may not be reflected in this version. For the definitive version of this publication, please refer to the published source. You are advised to consult the publisher's version if you wish to cite this paper.

This version is being made available in accordance with publisher policies. See <http://orca.cf.ac.uk/policies.html> for usage policies. Copyright and moral rights for publications made available in ORCA are retained by the copyright holders.



Sensorized robotic sphere for Large Exterior Critical Infrastructures supervision

Juan David Hernández^{*1}, David Sanz¹, Gonzalo R.
Rodríguez-Canosa¹, Jorge Barrientos¹, Jaime del Cerro¹, and
Antonio Barrientos¹

¹Centre for Automation and Robotics UPM-CSIC

January 17, 2016

Abstract

The surveillance and inspection tasks in Large Exterior Critical Infrastructures (LECIIs) have arisen as critical processes. More complex challenges are now present, and the traditional approaches are sometimes obsolete for facing these new menaces. The present paper proposes an alternative system -a mobile sensors, spherical shaped- that provides a flexible, versatile and reliable way to perform measurements. Even more, thanks to its original traction method (based on Center of Gravity -CoG- destabilization), the system has result as an all-terrain vehicle that guarantees a safe and friendly interaction with the environment. It has been widely tested, verifying as

^{*}juandhv@etsii.upm.es

well the accurate acquisition performance, resulting this system as a suitable sensing and monitoring alternative.

1 Introduction

Critical Infrastructures (CI) are those physical and information technology facilities, networks, services and assets which, if disrupted or destroyed, would have a serious impact on the health, safety, security or economic well-being of citizens or on the effective management and governance of a country [?]. Their security and effective surveillance have become challenging requirements that must be taken into account when designing the operation and integrated functioning of the essential elements of the installation.

Exterior Critical Infrastructures (ECIs) present common characteristics, mainly their size (i.e., usually quite large) and location (i.e., commonly far away from highly populated areas), that permit to group and study their security and surveillance under a common scheme. Power plants, communication centers, energy production plants, dangerous material storage facilities and dams are examples of ECIs.

In most ECIs the security and surveillance tasks have been usually undertaken by a combination of static sensors (cameras, movement detectors, etc.) and human guards. In this context, the use of robotic solutions is becoming quite popular due to their inherent advantages in terms of: *i*) intensification, *ii*) larger perception range, *iii*) greater mobility and adaptability and *iv*) risk reduction for human guards. From these factors, the reduction of risk to human guards has become the main thrust for the implantation of these type of surveillance solutions.

Different types of robots and robotic solutions have been designed and used according to specific scenarios. From the late 80s, when the IRIS robot performed inspection tasks in nuclear plants [?, ?], to current commercial robotic surveillance solutions (e.g. the patrolling of South Korean's Pohang prison by RoboGuard [?]), security robots have been successfully deployed. In this context, in the most advanced sensing systems not only ground robots [?, ?, ?] but unmanned aerial vehicles (UAV) have been incorporated as part of security and surveillance multirobot systems [?, ?, ?]. Examples of these platforms are the AirRobot's AR100-B ¹ and Astec's Pelican ² UAVs.

Nevertheless, the particular Exterior Critical Infrastructure conditions make difficult to provide a generic solution: uncertain terrain conditions, presence of humans, different significant magnitudes or great variability in the area-to-cover supposes a real challenge. Even more considering that some facilities could suppose a risk for the own robot safety (e.g. radiation in nuclear plants)). Therefore a mobile monitoring solution for general ECIs would require the incorporation of robotic vehicles able to displace themselves on rough terrains over long distances, carry different payloads and to avoid collisions and dangers. In this scenario spherical robots arise as a perfect compromise capable of addressing most possible contingencies, carry out. Although rarely used for this type of applications [?], it is our belief that their use may be an effective alternative to more classic robots.

The main objective of this work is to propose a generic surveillance system -based on spherical robots- able to measure the required magnitude in any kind of ECI scenario. In this sense, the present paper exposes this

¹<http://www.airrobot.com/index.php/products-28.html>

²<http://www.asctec.de/asctec-pelican-3/>

work. It is organized as follows. Section 2 outlines the specific requirements of a surveillance robot for this infrastructures and evaluates the possible solutions to the problem. Section 3 presents and analyzes the available spherical robots solutions. In Section 4, four experiments are presented and discussed. Finally, section 5 summarizes the conclusions and future work in this matter.

2 Problem outline and solution assesment

This section presents a study of the characteristics of a ECI, as well as a summary of the requirements of a surveillance robotics sensing platforms working in this environment. Finally, different robotic platforms for these applications are critically studied and compared.

2.1 General Characteristics of a ECI

ECIs present a set of characteristics that justify the incorporation of a specifically designed multirobot system (*MRS*) for security and surveillance. Safety and robustness are the main requirements for the use of robots in these sensitive facilities, where the failure of any subsystem might cause serious damages to the facility and its surroundings. Thus, reliability of the robotic solution must be warranted by all means.

The main ECI features to be taken into account to design a surveillance MRS solution are the following:

- **Location:** The CI locations can be quite different, but in general they are placed away from population centers. Very often, these facilities will be found in industrial areas in the suburbs of the cities,

as well as in zones far away from the urban nuclei.

- **Size:** They are usually large facilities with varying sizes from 60 to 3000Ha, depending on the type of ECI.
- **Surface:** In general, part of the whole installation grounds will be asphalted with tracks, passages or streets to move through its interior. Depending on the size of the facility, these ways or roads will be of a greater or smaller size and will be paved in a better or worse way. In installations integrated in rural terrains placed far away from urban areas, the ways inside the installation will usually be made of compacted soil.
- **Inclination:** Generally, there will not be pronounced slopes within the facility, although there can be several height levels. Most often in the installation there will be two or more parts placed at quite different levels. In this case, the parameter “slope” must be taken into account to define the traction system of the robots.
- **Internal Elements:** Main internal elements in this type of infrastructures are large storage buildings and loading docks. The presence of human operators and other machines and vehicles should be also expected.

The previously mentioned characteristics describe general characteristics of a ECI. Focusing in different types of infrastructures some differences can be noticed. A summary of the characteristics for different types of ECI is shown in Figure 1.

The surveillance of any ECI concerns two main aspects: the security against external threats and the security against internal malfunctions. For both of this tasks is important to have agile sensing platforms capable of

Table 1: Summary of characteristics of different types of CIs

ECI Type	Location	Size	Surface	Inclination	Internal Elements
Basic	Non-Urban	100-3000Ha	Asphalt	Small	Multiple
Solar	Non-Urban	60-120Ha	Sand and soil	Moderate	Heliostats
Nuclear	Non-Urban	60-100Ha	Irregular soil	Flat	Towers
Airport	Semi-Urban	3000Ha	Compacted soil	Flat	Control tower
Harbor	Urban	600Ha	Asphalt	Flat	Containers
Dam	Non-Urban	500-2000m	Asphat	Great Slopes	-

moving through the whole facility without disturbing its normal operation. In addition, other important inspection tasks of the robots refer to the monitoring of the damage of internal elements (lamps, fences, etc.) or vegetation growth monitoring.

This paper is focused on the requirements of a robotic sensing platform to monitor different parameters along the infrastructure. These requirements are presented in the next section.

2.2 Requirements of robotic sensing platform for ECI surveillance

The most important characteristic to design a robot intended for an Exterior Critical Infrastructure monitoring are its reliability and robustness. They imply that the robot must remain stable and provide the same performance regardless of the external conditions, both at the hardware and software levels.

The ECIs location, typically in remote scenarios, may result in exposing the robots to hard conditions such as heavy rains, extreme temperatures or dusty winds. It can also be expected that a part of the installation is made of rough terrain and that the different weather conditions along the different seasons of the year alter significantly the conditions of the environment. For example, there can be snow or ice sheets in winter, puddles or muddy areas in autumn, or sandy and crumbly grounds during summer.

All these factors affect directly the design of the movement mechanism, probably the most important element of the robot. Moreover, the traction system needs to be versatile and able to displace the robot along different types of surfaces, from urbanized even terrains where the robot might slide to rough non-structured surfaces. The traction system should allow the robot to follow trajectories with sharpen angles and narrow passages.

Due to the size of the infrastructure, another important factor is the autonomy of the sensing platform. These robotic platform should be able to perform continuous monitoring for several hours without recharging.

The internal elements of the infrastructure also affect the choice of the traction system and the general design of the robot. The chosen vehicle should be able to perform its inspection operation ensuring both its own safety and the safety of the rest of the elements. Since human workers are to be expected in the facility, a friendly interaction system is necessary. Thus, the robot should be able to detect and avoid static and mobile objects or, in case of collision, not injure the human operators or damage any part of the infrastructure.

Additional minor considerations as the ability of the cameras of not

being affected by dust when taken images should also be considered in the design of a robotic solution.

In summary, the most important characteristics of robotics sensing platform are: robustness, ability to move in different terrains, autonomy and safe interaction with the environment.

2.3 Analysis of present solutions

The classical solution to detect radioactive leakages, present in all nuclear facilities, is a network of sensors distributed along the whole installation. The main disadvantage of this method is that, to detect a radiation leakage, it must be significant enough to be detected by the nearest sensor. Small or localized leakages would remain undetected for a long period of time if the leakage is located far from a sensor. Increasing the number of sensor to a point where this factor is no longer significant would be extremely expensive and inefficient.

A more efficient approach would be to use a robotic solution. Different types of solutions with different configurations and characteristics have been studied and evaluated with regard to their use for localized radioactive leakage detection in a NWR. To systematically perform this analysis different parameters have been defined according to the requirements specified in section 2.2. These characteristics are: mobility, maneuverability, robustness, autonomy, payload capacity, action range, measurement accuracy and interaction with the other elements of the installation.

- **UAV:** These vehicles present a high level of mobility, but their low autonomy, small payload capability and poor maneuverability makes them unsuitable for the selected application. Furthermore, since the

leakages mostly affect at the ground level, the advantages of having an aerial perspective are lost as the UAVs would have to fly close to the ground for a reliable detection. Other problems with this type of vehicles are their inability to operate in extreme meteorological conditions (i.e., heavy rain or gusty winds), special requirements for take-off and landing and security concerns in their interaction with the other elements (i.e., dangerous situations for the human operators in case of robot malfunctions). Their expected high initial and current maintenance costs are additional factors that preclude the use of these vehicles for this application. UAVs can be classified in two different types with specific characteristics.

- *Rotational Wing UAV*: This type of UAVs have usually a slightly smaller payload capacity and robustness but a higher maneuverability.
- *Fixed Wing UAV*: The main advantage of this type of UAV is its higher action range and autonomy.
- **Large UGV**: The main problem of this type of units is their size, as large UGVs have low maneuverability and mobility and cannot fit through narrow passages. Although other characteristics of these vehicles, such as a large autonomy, big payload capacity, high robustness and high measurement accuracy, are very desirable for the intended application, the size limitation usually discards this type of robots for surveillance applications in MRW facilities.
- **Small UGVs team**: Using a robotic swarm of small simple robots is actually very suitable for this application. Its main advantages are the ability to perform simultaneous measurements in different parts

of the installation and the great maneuverability and mobility that present this type of robots. Their small size fulfills a critical requirement since it allows them to fit through narrow spaces and to follow sharp angled trajectories. Also, in case of collision, they would cause minimum impact to the other elements of the environment. Their main drawback refers to their limited payload capacity that imposes the use of small and light batteries, thus reducing their autonomy and their autonomous field of work.

- **Bio-inspired systems:** The main limitations of bio-inspired locomotion systems resides in the characteristics of are their movement systems (e.g., leg based or crawling methods) that, in comparison with other more conventional methods (e.g., wheeled propulsion), are usually highly power consuming and provide low velocities. The available commercial and laboratory-based bio-inspired platforms are still highly unstable and are unable to cover a large area in a reasonable period of time.

A suitable solution that combines great mobility and maneuverability together with an acceptable autonomy, high payload capacity and robustness is a robotic sphere similar to that presented by Seeman *et al.*[?] or by Zhan *et al.*[?]. The main benefits of this type of robots come from their shape and motion structure that minimize energy losses due to friction. Their spherical shape allows the robot to displace themselves along different terrains and surfaces (even water) with a minimum consumption of energy. The motion principle consists of a pendulum-based device that induces movement destabilizing the sphere. This principle is different than that of opposes other more traditional movement methods where a torque

momentum is responsible to generate displacement in wheels.

This type of movement generation, implying a minimum lift over the background surface, allows the robot to move without producing dust. This beneficial aspect of its operation is not significantly affected by the payload weight as long as it is balanced within the sphere. The shape of the robot and its relatively small size and low weight imply a friendly interaction with the environment since any collision would have a minimum effect on the other elements of the installation. Another advantage is the rapid recuperation of its attitude in case of destabilization; i.e., a recovery effect similar to that of tilting toys.

The same characteristics (i.e., shape, size and movement control) that are so advantageous with regard to the implementation of these robots in a NWR, have a negative impact in the robot control and navigational systems. Precise trajectories, locations or attitudes are difficult to define and follow, resulting some times in curvilinear uncontrolled trajectories. When static, the robot contacts the surface in a single point generally resulting in an unstable situation. Big obstacles would also be a problem. Nevertheless, these two limitations are not critical in the present scenario where huge obstacles are not expected and high accuracy in the attitude is not needed.

A critical comparison of the aforementioned vehicles solutions with respect to the use of the robotic sphere is summarized in Table 2.

In the next section the internal mechanism of the proposed robotic sphere is explained in more detail.

Table 2: Comparison of available solutions for radioactive leakages detection according to the following parameters: C_1 =Mobility, C_2 =Maneuverability, C_3 =Robustness, C_4 =Autonomy, C_5 =Payload Capacity, C_6 =Action Range, C_7 =Safe Interaction with other elements

	C_1	C_2	C_3	C_4	C_5	C_6	C_7
Sensor Networks	x	x	++	+++	x	++	+++
RW UAV	+++	+++	+	+	++	++	+
FW UAV	+++	+	++	++	+++	+++	+
Large UGV	+	+	+++	+++	+++	++	+
Small UGVs Team	++	++	++	++	+	+	++
Bio-inspired	+	++	+	+	+	+	++
Robotic Sphere	++	+++	+++	+++	+	++	+++

3 System outline

Considering the aspects mentioned above, a rolling robot has been proposed as a solution to fulfill successfully all the operational requirements. Its maneuverability, versatility, and capacity to recover from collisions are characteristics that make this type of robot suitable for the particular application studied in this article. Throughout this section, the main features of the system are explained, including the mathematical concepts involved in its operation, as well as the main mechanical and electronic design aspects of current prototypes.

3.1 Basic principle of locomotion

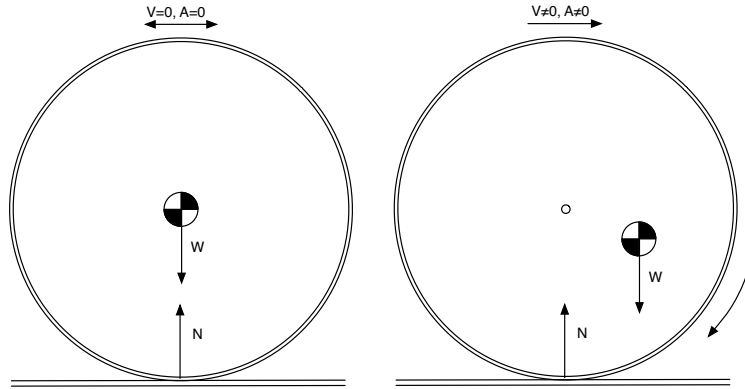
The objective of this work is to present a rolling robot with a spherical shape, called "ROSPHERE" (RObotic SPHERE), as an alternative mobile platform to perform monitoring and inspection tasks. In contrast to other mobile robots (e.g. walking systems) whose basic locomotion principle is the system stability; movements in robotic spheres are induced by instability. Another consequence is that, due to its regular shape, the robot

recovers easily from collisions so that, regardless the direction of the impact, the robot always tends to fall into a recoverable configuration. Herein, in order to have a global view of the robot capabilities, we will analyze the internal mechanism which endows the system with these characteristics.

Let us consider first a sphere where mass is uniformly distributed mass. In this case, the center of mass is coincident with the geometrical center. Also, if the sphere is in contact with a non-lifted surface, the projection of the center of mass over the surface will be at the contact point. Under these conditions, the sphere will have no acceleration nor velocity in any possible direction (i.e., the sphere is at rest) (see Figure 1.a).

If a sphere is built by using a non-uniform material, its center of mass would not be located at its geometrical center. In this case, when placing the sphere on a flat surface, the projection of the center of mass over that surface will not coincide with the contact point and it will overturn until reaching an equilibrium configuration (see Figure 1.b).

Figure 1: Basic principle of motion. The projection of the center of mass over the surface may define whether the sphere has non-zero acceleration and velocity. (a) Balanced configuration. (b) Unbalanced configuration.



Finally, if the distribution of mass, i.e. the position of the center of mass, can be defined arbitrarily, the spherical system would be able to self-induce

movement in any possible displacement direction (i.e. a holonomic system). That is the basic principle of locomotion in a robotic sphere, a spherical-shaped vehicle that includes an internal mechanism which permits to vary the position of the center of mass and, therefore, to self-induce motion.

3.2 State of the art: concepts and first prototypes

Even though robotic spheres are not widely used as mobile platforms, it is possible to find in the literature quite significant contributions to the problem, as well as new, concepts and prototypes proposals. Initially, research activities were focused on validating physics concepts. In this regard, some authors have proposed different approaches where the main objective was to create a mechanical system that permits to locate the center of mass of a sphere and, therefore, to self-induce motion. Nowadays, there are basically five alternatives to reach this objective [?].

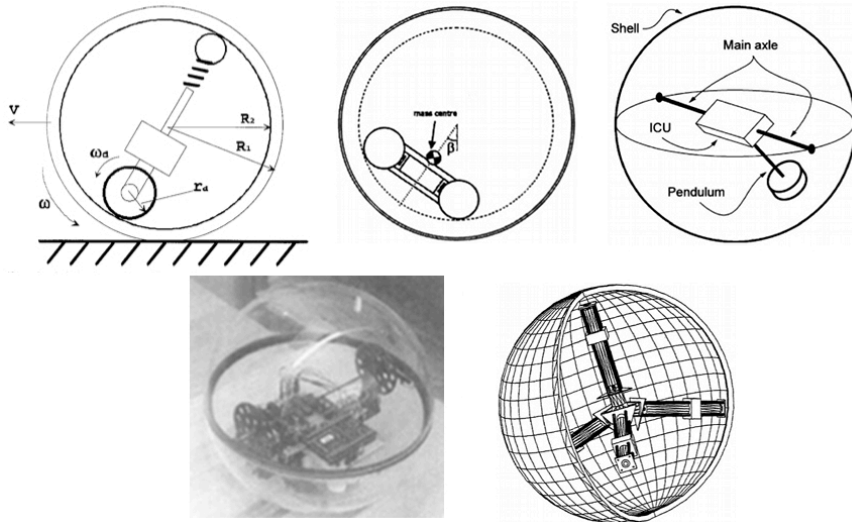
The first concept is known as *spring central member* [?, ?]; this alternative has a central body that includes a driven wheel on one of its ends and a passive wheel on the other, with a spring that guarantees contact of both wheels and the spherical shaped body (see Figure 2.a). Its main disadvantage is the loss of energy due to friction between both wheels and the sphere. A similar concept, known as *car driven* [?, ?, ?], utilizes an inside vehicle to induce motion. However, this mechanism does not guarantees contact between the vehicle and the sphere (see Figure 2.b), what constitutes an important drawback, specially when the sphere is moving along a surface with depressions and bumps. In this case since the contact, and consequently the control over the system, may be lost.

Another alternative relies on a ballast mass, a concept that has two

variants. The so called *ballast mass with fixed axis* system utilizes an inner pendular mechanism that consists of two rotational degrees of freedom (DoF) [?, ?, ?, ?, ?, ?, ?, ?, ?, ?]. The first one rotates around a fixed transverse axis and the second one around a longitudinal axis (see Figure 2.c). The second variant is designated as *ballast mass with moving axis*. It also has an inner pendular mechanism, but in this case with an additional DoF that permits to move the main axis (see Figure 2.d).

These prototypes are examples of non-holonomic systems, since the vehicle has to start moving forward or backward in order to make turns, as it does not have the capacity to turn over itself in all possible directions. An alternative to reach the set of characteristics of holonomic vehicle is based on the *mobile masses* system [?, ?]. Prototypes using this concept take profit of the movement of masses along radial axes to modify the position of the center of mass (see Figure 2.e).

Figure 2: Alternative mechanical systems used to self-induce motion in a robotic sphere. (a) Spring Central Member. (b) Car Driven. (c) Ballast Mass Fixed Axis. (d) Ballast Mass Moving Axis. (e) Mobile Masses.



Besides these theoretical concepts, different authors have developed

robotic spheres for quite different areas of applications. Perhaps the most cited and ambitious application of robotic spheres has been the one proposed by Zhan *et al.* [?] to explore unstructured and unknown environments by exploiting their robustness and versatility. Meanwhile Bruhn *et al.* [?] or Michaud *et al.* [?] have proposed their use for planetary exploration. Other fields of application that could benefit from these characteristics are security, surveillance and inspection [?], whereby robotic spheres are equipped with sensors and cameras in order to facilitate the robot teleoperation.

Last but not least, since one of the principal requirements of service robots is the capacity of harmless interaction with people, robotic spheres have also been used in this area where have demonstrated this attribute. Thus, for example, Michaud *et al.* [?, ?] have used a robotic sphere equipped with the necessary control routines and sensors to measure child development. Children used the robot as a toy while the system acquired information to evaluate their development. Finally, more academic contributions presenting robotics spheres to study kinematics, dynamics and control of non-holonomic systems can also be found in literature [?].

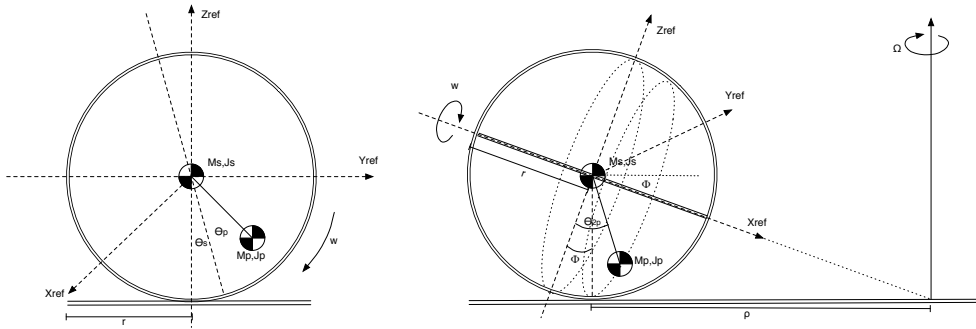
For the purposes of the present application, the selected mechanical alternative has been the *ballast mass with fixed axis* (Figure 2.c). This mechanical option provides a fixed point (at the ends of fixed axis) where external sensors can be located. Alternatives that include internal active wheels (Figures 2.a and 2.b) were discarded because of their poor energetic efficiency. The following sections discuss different aspects related to the selected mechanism, such as physics model, mechanics, and hardware and software architectures.

3.3 Mathematical model

In this section we present a synthesis of various available mathematical models that include the basic physics concepts needed to understand the system behavior [?, ?, ?]. Since the main objective of this article is to contextualize the use of a robotic sphere in a real environment, we do not present a novel mathematical approach, which has been the subject of earlier contributions focusing on the development of mathematical and physics models of robotic spheres. Further information and more complex considerations can be found in [?, ?, ?, ?, ?, ?].

The present analysis separates the system dynamics into two parts [?]. A part, inducing forward and backward motion (i.e., *driving dynamics*), is related to the action applied to the first DoF. The second part (i.e., *steering dynamics*) makes that the sphere turns and corresponds to the effect generated by the second DoF. The combined effect of these two parts endows the sphere with the characteristics of a non-holonomic vehicle.

Figure 3: Decoupled dynamics analysis. Equations are separated in motion induced by each actuator. (a) Model for forward/backward movements. (b) Model for steering movements.



These two parts of the mathematical model are described with more detail in the following sections.

3.3.1 Driving dynamics

This section summarizes the equations of motion for the driving dynamics developed through a Lagrange formulation. A deeper analysis can be found in [?], where a general case of a motion induced by a mobile mass inside a spherical body is explained. Based on this formulation, Nagai *et al.* [?] presented an extension for an inner pendulum-based system. Another alternative to a Lagrange formulation is a Newton formulation, firstly proposed for a robotic sphere by Halme *et al.* [?] in 1996.

Assuming that the system is only able to move in one plane (i.e., forward and backward), the robot can be modeled as a two-rigid-body system with a single DoF between them, as it is shown in Figure 3.a. The resulting Lagrange equations can be calculated as follows.

The Lagrangian is defined in Equation (1), where $K = K_s + K_p$ and $U = U_s + U_p$ are the kinematic and potential energies of the sphere and the pendulum respectively.

$$\mathcal{L} = K - U \quad (1)$$

The kinematic and potential energy terms are described in (2).

$$\begin{aligned} U_s &= 0 & U_p &= -M_p g l \cos(\theta_s + \theta_p) \\ K_s &= \frac{1}{2} M_s \left(r \dot{\theta}_s \right)^2 + \frac{1}{2} J_s \dot{\theta}_s^2 & K_p &= \frac{1}{2} M_p \left[\left(r \dot{\theta}_s - l \cos(\theta_s + \theta_p) \left(\dot{\theta}_s + \dot{\theta}_p \right) \right)^2 + \right. \\ & & & \left. + \left(l \sin(\theta_s + \theta_p) \left(\dot{\theta}_s + \dot{\theta}_p \right) \right)^2 \right] + \\ & & & + \frac{1}{2} J_p \left(\dot{\theta}_s + \dot{\theta}_p \right)^2 \end{aligned} \quad (2)$$

The Lagrangian motion equations can be obtained by differentiating Equation (1) as it is shown in (3), where τ is the motor torque and τ_f the friction torque between the sphere and the terrain.

$$\frac{d}{dt} \left(\frac{\partial \mathcal{L}}{\partial \dot{\theta}_p} \right) - \frac{\partial \mathcal{L}}{\partial \theta_p} = \tau \quad \quad \frac{d}{dt} \left(\frac{\partial \mathcal{L}}{\partial \dot{\theta}_s} \right) - \frac{\partial \mathcal{L}}{\partial \theta_s} = -\tau + \tau_f \quad (3)$$

Substituting the expressions in Equation (2) into Equation (3) and grouping into a matrix equation, the equation of motion for a general rigid-body system can be written in the canonical form, as shown in Equation (4). In this equation $M(q)$ is the mass matrix, which depends on the system configuration; $(q = [\theta_s, \theta_p]^T)$ and $C(q, \dot{q})$ are the Coriolis terms (speed-dependent); $G(q)$ are the gravity terms; F_{ext} are the external forces (friction); and τ are the forces applied by the actuators.

$$M(q) \ddot{q} + C(q, \dot{q}) + G(q) - F_{ext} = \tau \quad (4)$$

3.3.2 *Steering dynamics*

In this section, the second DoF (θ_{2p}) is analyzed. This angle is responsible of inducing the robot inclination, and is considered to be the robot roll angle (Φ), as shown in Figure 3.b.

Assuming that the robot moves with a low velocity, there is an equilibrium between force and torque (including the centrifugal force of steering) and, as a result of it, the sphere follows a circumference with radius ρ and a angular velocity Ω . This assumption is important since a robotic

sphere steering with high speed implies that Coriolis and centrifugal forces may affect pre-defined trajectories. A complete analysis for a high-speed conditions can be found in [?, ?].

The radius of the turning circumference can be calculated as shown in Equation (5), where r is the radius of the sphere.

$$\rho = \frac{r}{\tan(\theta_{2p})} \quad (5)$$

The angular rate for steering (Ω) can be calculated as shown in Equation (6), where ω is the angular velocity of the robot ($\dot{\theta}_s$).

$$\Omega = \omega \cdot \sin(\theta_{2p}) \quad (6)$$

3.4 Mechanical design

ROSPHERE has an inner two-degree-of-freedom pendulum. Figure 4 shows a general concept of the mechanism, including its main parts: *a)* the spherical shaped body, *b)* a fixed main axis, *c)* a central unit or ICU (Internal Control Unit, as defined by other authors) and *d)* the ballast or hanging mass. The first DoF allows the rotation of the ICU, and consequently of the hanging mass around the fixed axis. For this rotation, a continuous rotation actuator with no angle limit is needed. The second DoF, on the other hand, has a limited rotation range, which ideally should be 180°. However, this rotation is in practice mechanically limited. For the first prototypes, two identical servos (HS-7954SH ³) were selected, one of which was modified to be used as a continuous rotation servo.

³<http://www.hitecrcd.com/products/digital/hv-ultra-premium-digital/not-set.html>

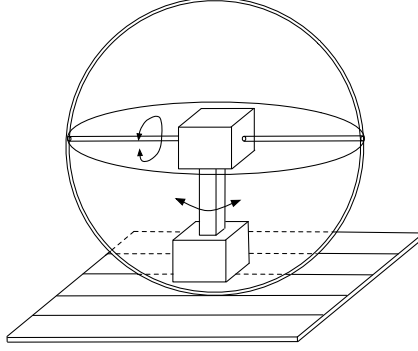


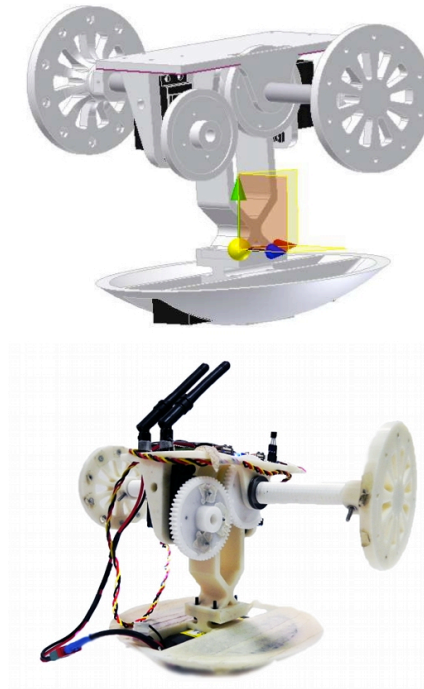
Figure 4: ROSPHERE, internal ballast mechanism with two DoF. The first one rotates around a fixed transverse axis, while the second one around a longitudinal axis.

A first prototype, ROSPHERE v0.1, was designed to assess motion capabilities and physics concepts. A ferret ball was used as the main spherical body. This ball can be separated in two hemispheres with caps where the main aluminium axis was fixed. All the other parts of the model, including the pendulum and the ICU were designed in a 3D modeling software (Inventor®) and built using a 3D plastic printer.

After evaluating the results obtained with the first prototype (v0.1), some design flaws were detected that produced a certain instability of the prototype and the addition of a certain amount of useless mass to the pendulum. As explained in Section 3.3, another important factor is the angle required to induce motion to the system. This angle depends on different factors, from which the most important one regarding the mechanics is the relative position of the center of mass (CM) with respect to the geometrical center. In other words, the further the CM is from the geometrical center, the smaller the angle needed to produce motion. A second prototype, named ROSPHERE v0.2 and shown in Figure 5, includes lighter plastic pieces enabling that the CM is lowered. This could be verified before

printing the new parts, by comparing the position of the center of masses of both prototypes as calculated by Inventor®. Besides, to stabilize the system in stationary and moving states, the servos were located in positions making that the CM is as closer as possible to the pendulum body axis.

Figure 5: Internal mechanism of ROSPHERE v0.2 uses lighter plastic pieces to lower the CM. (a) Mechanism designed in Inventor®. (b) Real mechanism.



3.5 Hardware and Software architectures

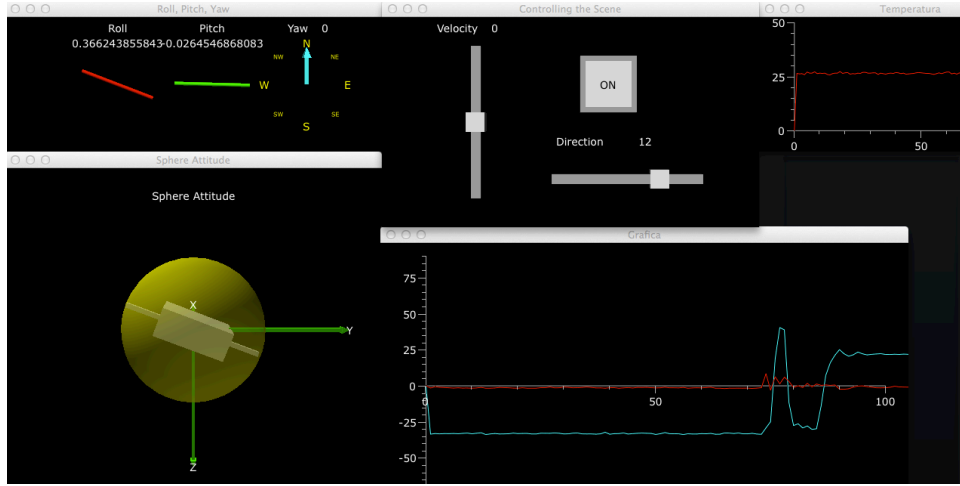
On the other hand, ROSPHERE is equipped with all necessary resources to behave as an autonomous vehicle. This point is nowadays at the core of the research efforts in this topic. In the earlier beginnings, the system was supplied with an embedded computing system composed by a Robovero ⁴ (a Gumstix expansion board) and a Overo Fire ⁵ (a Gumstix embedded computer) that initially used Ångström Linux initially. At present time,

⁴https://www.gumstix.com/store/product_info.php?products_id=262

⁵https://www.gumstix.com/store/product_info.php?products_id=227

ROSPHERE v0.2 has WiFi, Bluetooth and Xbee as communication alternatives. Furthermore, it also includes other sensors, such as an Inertial Measurement Unit (IMU), a GPS, a temperature and relative moisture sensors. Some of these sensors can be visualized through a Graphical User Interface (GUI) that is part of the remote station of the robot (Figure 6).

Figure 6: Remote Station. Graphical User Interface (GUI) used in teleoperation mode. It permits to control each DoF and visualize the values and states of sensors, including the IMU (Roll, Pitch, Yaw), temperature and relative moisture.



Robovero is an electronic board for robotic applications ⁶ and the main board of the robot's ICU. One of its most important features is the inclusion of a microcontroller, a 9-DOF IMU (3-DOF gyroscope, 3-DOF accelerometer, 3-DOF compass), power electronics to connect motors, and a USB HUB. Robovero has a firmware that permits the microcontroller to receive commands through a USB connection. The commands allow read and write I/O devices (such as I2C, UARTs, SPI, PWM, A/D, etc.). Therefore, Robovero itself is not an embedded computing system, but can be considered a peripheral board. However, microcontroller's commands are

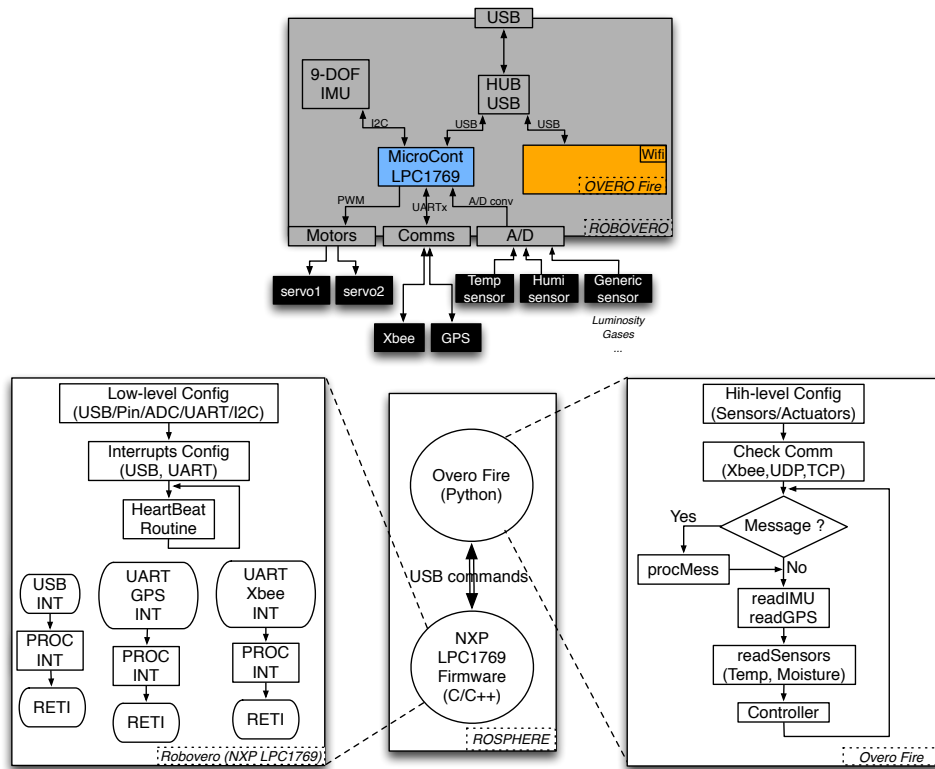
⁶<http://robovero.org/>

received through USB, either from an external computer, or from a embedded one, like overo fire. Finally, the whole system (robovero+overo) is an embedded computing system which, together with the actuators and sensors, complete the hardware architecture of the system (see Figure 7.a).

The software system architecture can be divided into two main parts. A high level computation layer that must interpret primitive movements commands in teleoperation mode and generate the respective actuators commands or, alternatively, to navigate autonomously according to high level orders and the information provided by the sensors. On the other hand, there is a low level computation layer that is in charge of collecting (reading) information from sensors and to control actuators. Both, high and low layers are directly related to hardware architecture, as the high-level corresponds to Overo Fire programming, while the low-level corresponds to Robovero's microcontroller (See Fig. 7.b).

Overo embedded computer has Linux as operating system. In a first stage of tests, Linux Ångström distribution was used to verify communication capabilities (WiFi, Bluetooth, Serial, Xbee), as well as for internal communication to Robovero's processor through USB connection. Over Linux, High-level programming is coded in Python and uses an API that wraps Robovero USB commands. Even though Python may be considered a non time efficient programming language, it is used to control the execution flow of the main application, while time demanding parts are coded in C/C++ as extension modules. Robovero's processor, on the other hand, runs a firmware that basically is checking USB port in order to receive commands and interpret them. The original firmware was designed to read ports (I2C, UART, AD, etc.) using a polling mode. However, the firmware

Figure 7: ROSPHERE hardware and software architectures. In (a), the hardware architecture that presents the connection between the high-level and low-level processors, sensors and actuators. In (b), the software architecture that presents the low-level and high-level computation layers.



has been modified to accept interruptions.

4 Experimental Results

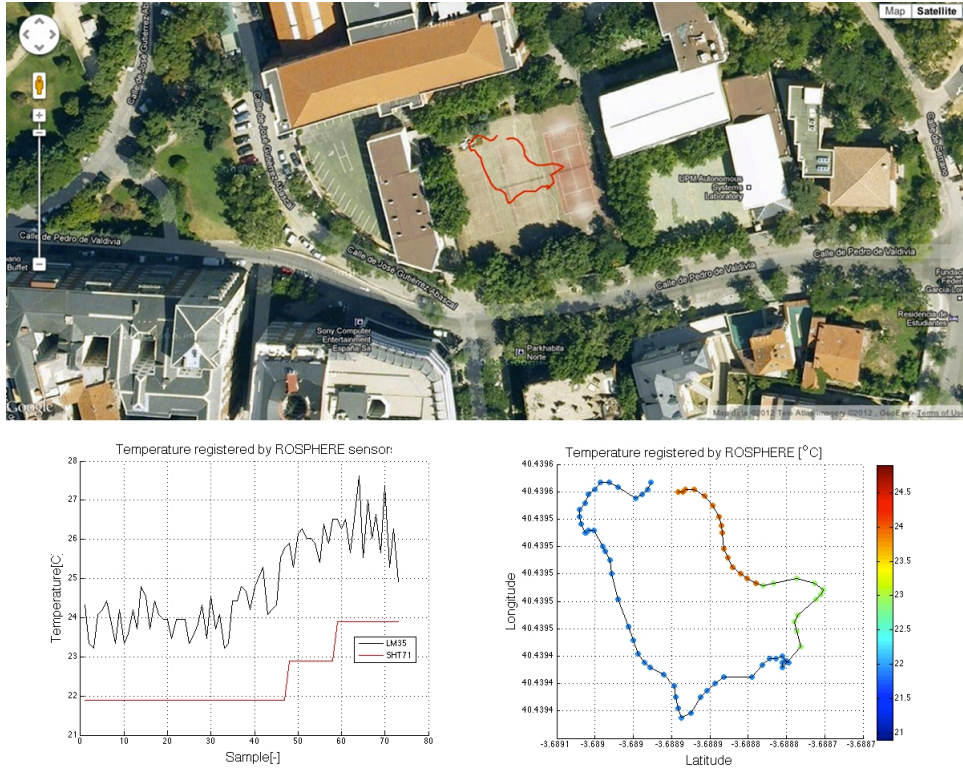
To validate the design and verify the capabilities of our prototype, the system needs to be thoroughly tested. A large set of experiments was designed and executed to assess the system capabilities both individually and from a global point of view. In the next subsections, four different experiments are presented each one focused on a particular aspect of the system.

4.1 Experiment 1: Acquisition Process

The first scenario has been designed to validate the main concept of the system: the acquisition process and the ROSPHERE performance as a mobile sensor. Along this line, experiment 1 has assessed the measurement ranges, including not only the maximums and minimums of the sensors but also their real acquisition rate. As well, data-location correlation and the orientation (pose) dependency have been also evaluated.

It was carried out at the University facilities (see Figure 8), defining a fenced and controlled area in the sports area. Over it, several electric heaters were spread, in order to be able to set the temperature in an artificial way. Figure 8.b illustrates this operation, where it is possible to appreciate that the temperature in this area (upper right zone) is higher than the mean one. Furthermore, in order to have a reference value, an external and parallel measurement was performed with a precision thermometer along the path. It allowed to verify a maintained 11°C offset in

Figure 8: Experiment 1: Mobility and acquisition test in the UPM facilities. Several test were performed in a controlled area to verify the measurement accuracy and the mobility capabilities. (b) Comparison of the temperature acquired by both sensors ($^{\circ}\text{C}$). (c) Temperature along the path covered. ($^{\circ}\text{C}$).



the LM35 temperature sensor and 9°C difference in the SHT21. This error was estimated to be self-induced, provoked by the electronics and engines internal heating. Nevertheless, it has been corrected given that the tests have shown that it could be considered almost constant in steady state (around 150s after the startup).

Moreover, these tests allowed to integrate both temperature sensors: while first one (SHT21) revises and attenuates the second's noise, this second one (LM35) contributes with a higher accuracy (see Figure 8.c). The combination of both values provides a system with a <1 °C resolution. The results of this experiment have also allowed to define the ROSPHERE's maximum speed that guarantees a suitable acquisition process, as well as the minimum accuracy expected.

4.2 Experiment 2: Safe interaction

The next experiment was designed to test the systems capability to safely interact with the environment and with people. In order to prove that the sphere is able to work in a crowded environment with operator, machinery and dangerous materials, the system was tested in a park. This was a good testbed of a non-structured environment with different numerous mobile elements (i.e., persons, bicycles, cars...). The main objective was to test navigation capabilities and to evaluate the impact on the environment. Other tests performed during this experiment included external perturbations (i.e. kids trying to play with the sphere) and minor collisions with static elements such as walls or trees. Figure 9 illustrates a safely interaction occurred during this experiment.

During this experiment other measurements were taken, although they

Figure 9: ROSPHERE safely interacting with a kid in *El Retiro* park in Madrid, Spain.

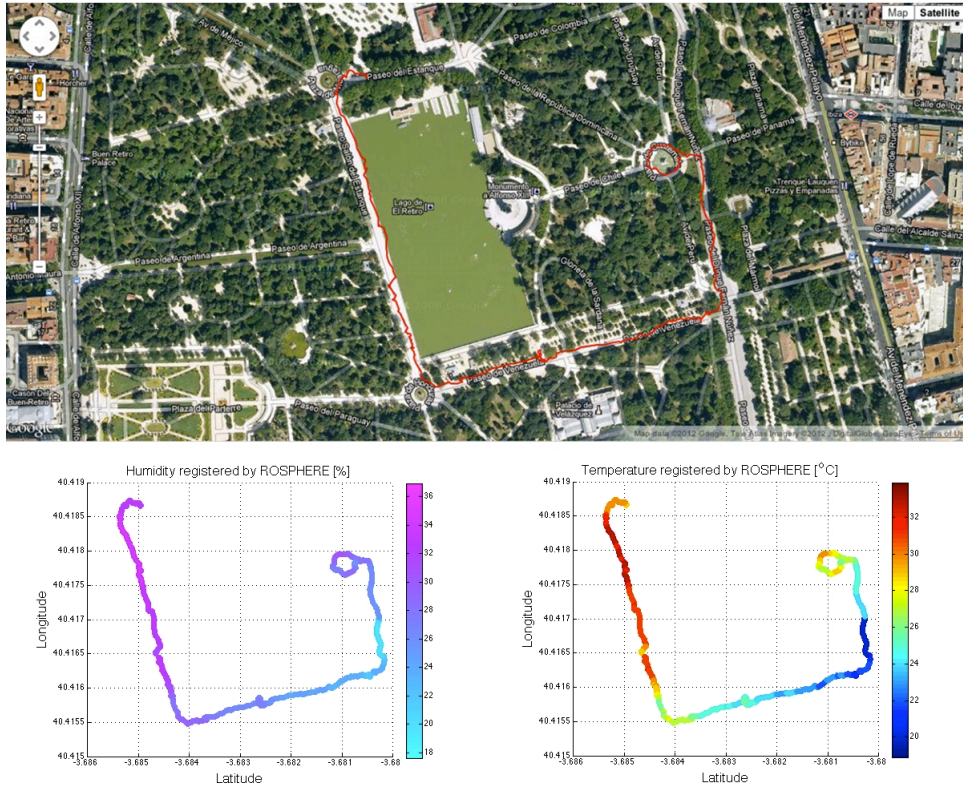


were not the main objective of the test. In this case, correlated measurements of temperature and humidity were taken. It may be noted that the relative humidity rises near the areas where water was present, in this case around the lake and also around the fountain the robot circles. In relation to the temperature, the values measured were higher around the lake because this area was more exposed to the sun than other along the route where the robot was protected by trees and vegetation.

4.3 Experiment 3: Terrain Conditions

During the multiple test carried out to assess the robot capabilities, the performance of the sphere in different terrains was also tested. Traction in different surfaces was observed. Our conclusions are that, although the velocity of the robot changed according to the terrain, ROSPHERE surpassed the expectations in any terrain. The sphere was tested in asphalt, gravel, sand and grass as shown in Figure 11. As mentioned before the main differences in the performance were more noticeable in the velocity and in the battery consumption, but the robot never got stuck or needed help

Figure 10: Experiment 2: Comparison between humidity-temperature in relation with the navigation (in *El Retiro* park in Madrid, Spain). (b) Humidity along the path covered (%). (c) Temperature along the path covered ($^{\circ}\text{C}$).



to continue moving effectively qualifying it as all-terrain robot.

Figure 11: Experiment 3: Movement and performance test under different surfaces and terrain conditions. (a) Sandy beach. (b) Grassy park. (c) Earthy crop. (d) Pavement.



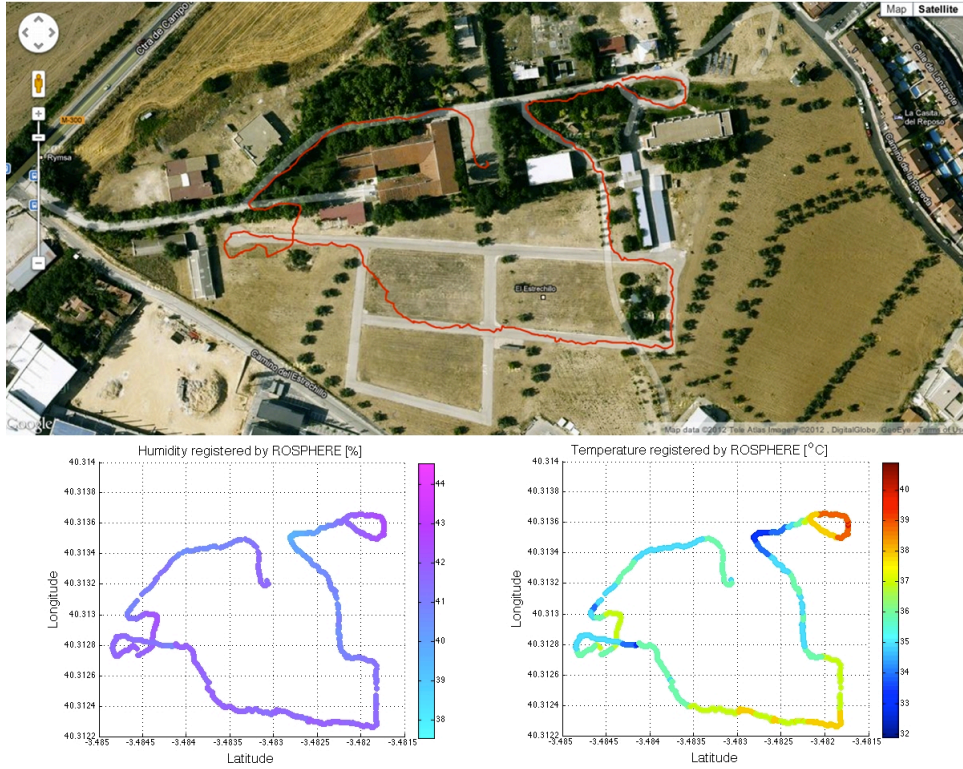
4.4 Experiment 4: Global Performance Test in ECI conditions

Finally, a global performance experiment was carried out in an Exterior pseudo-Critical Infrastructure: the Automatic and Robotic Center facilities in *Arganda* (Madrid). It has a fenced perimeter and includes both asphalted and rugged pathways. Another feature that made this installation suitable for this test was the constant presence of operators and both autonomous and driven vehicles.

During this test, temperature and humidity were measured. Figure 12 shows the map with the robot route as well as the temperature and humidity represented by a colored line. Expected values were obtained as temperature was lower in the areas where more trees were present.

This experiment also validated the last advantage of the spherical robot: its autonomy. The test was repeated three times, taking around 20 minutes each experiment. At the end, the remaining battery was higher than 40% validating the long autonomy assertion.

Figure 12: Experiment 4: Full simulation of a NWR facility in the CSIC installation in Arganda del Rey (Spain). Test of safety navigation, data acquisition and surveillance task. (b) Humidity along the path covered (%). (c) Temperature along the path covered ($^{\circ}\text{C}$).



5 Conclusions and future work

As stated throughout this paper, critical infrastructures have a crucial role for governments and companies. Due to this, in this work, the most relevant requirements for the surveillance of these scenarios have been analysed in detailed. In conclusion, a big research effort has to be made in order to improve the surveillance of these scenarios.

Currently, the most common solutions are combinations of static sensors (i.e., cameras and motion detection) and human guards. Unfortunately, these systems are generally tailored and not flexible enough. Modern multi-robot systems (aerial and ground) devoted to perform surveillance would improve this situation.

This paper presents the main aspects related to the design, construction and implementation of ROSPHERE, a spherical shaped robot that combines the reliability of the wheeled robot with the flexibility and versatility required to operate in different types of terrains. Due to this, it turns out to be an excellent candidate to be a part of a heterogeneous robotic team for surveillance.

These features are mainly achieved due to its original movement based on CoG destabilization instead of using friction-based movement. Additionally, its shape and weight prevents ROSPHERE from damaging the environment or people, being able to continue with its moving and sensing capabilities after collisions or even small falls.

However, some issues have to be addressed in order to fulfil fully autonomous operation and integration into a heterogeneous system. Thus, in order to improve the control performance, the addition of a rotational speed sensor would allow to control the sphere in extreme slippery surfaces.

Furthermore, a wireless link for external sensors will enhance data accuracy and make the connectivity easier.

Finally, in order to make easier the integration of ROSPHERE into a complex system, an effort is being carried out so as to provide it with a standard connectivity by using a common framework such as ROS (Robot Operating System). This task becomes easier since it natively works using Ubuntu as its operating system.

Briefly, ROSPHERE have been validated as a suitable alternative for accurate measurements in critical infrastructures. It has been proved that it can be a good replacement for some tasks in ECI surveillance, as well as for outdoor scenarios in general.

Acknowledgements

This work has been supported by the Robotics and Cybernetics Research Group at Universidad Politécnica de Madrid (Spain), and funded under the projects “ROTOS: Multi-Robot system for outdoor infrastructures protection”, sponsored by Spain Ministry of Education and Science (DPI2010-17998), and the project ROBOCITY 2030 Project, sponsored by the Community of Madrid (S-0505/DPI/000235).

Figure 1: Basic principle of motion. The projection of the center of mass over the surface may define whether the sphere has non-zero acceleration and velocity. (a) Balanced configuration. (b) Unbalanced configuration.

Figure 2: Alternative mechanical systems used to self-induce motion in a robotic sphere. (a) Spring Central Member. (b) Car Driven. (c) Ballast Mass Fixed Axis. (d) Ballast Mass Moving Axis. (e) Mobile Masses.

Figure 3: Decoupled dynamics analysis. Equations are separated in motion induced by each actuator. (a) Model for forward/backward movements. (b) Model for steering movements.

Figure 4: ROSPHERE, internal ballast mechanism with two DoF. The first one rotates around a fixed transverse axis, while the second one around a longitudinal axis.

Figure 5: Internal mechanism of ROSPHERE v0.2 uses lighter plastic pieces to lower the CM. (a) Mechanism designed in Inventor®. (b) Real mechanism.

Figure 6: Remote Station. Graphical User Interface (GUI) used in teleoperation mode. It permits to control each DoF and visualize the values and states of sensors, including the IMU (Roll, Pitch, Yaw), temperature and relative moisture.

Figure 7: ROSPHERE hardware and software architectures. In (a), the hardware architecture that presents the connection between the high-level and low-level processors, sensors and actuators. In (b), the software architecture that presents the low-level and high-level computation layers.

Figure 8: Experiment 1: Mobility and acquisition test in the UPM facilities. Several test were performed in a controlled area to verify the measurement accuracy and the mobility capabilities. (b) Comparison of the temperature

acquired by both sensors ($^{\circ}\text{C}$). (c) Temperature along the path covered. ($^{\circ}\text{C}$)

Figure 9: ROSPHERE safely interacting with a kid in *El Retiro* park in Madrid, Spain.

Figure 10: Experiment 2: Comparision between humidity-temperature in relation with the navigation (in *El Retiro* park in Madrid, Spain). (b) Humidity along the path covered (%). (c) Temperature along the path covered ($^{\circ}\text{C}$).

Figure 11: Experiment 3: Movement and performance test under different surfaces and terrain conditions. (a) Sandy beach. (b) Grassy park. (c) Earthy crop. (d) Pavement.

Figure 12: Experiment 4: Full simulation of a NWR facility in the CSIC installation in Arganda del Rey (Spain). Test of safety navigation, data acquisition and surveillance task. (b) Humidity along the path covered (%). (c) Temperature along the path covered ($^{\circ}\text{C}$).